

# UPCommons

## Portal del coneixement obert de la UPC

<http://upcommons.upc.edu/e-prints>

---

Aquesta és una còpia de la versió *author's final draft* d'un article publicat a la revista *Building and Environment*.

URL d'aquest document a UPCommons E-prints:

<http://hdl.handle.net/2117/101974>

---

### **Article publicat / Published paper:**

Macarulla, M., Casals, M., Carnevali, M., Forcada, N., Gangolells, M. (2017). Modelling indoor air carbon dioxide concentration using grey-box models. *Building and Environment*, In Press. DOI: <[10.1016/j.buildenv.2017.02.022](https://doi.org/10.1016/j.buildenv.2017.02.022)>.

1 **Modelling indoor air carbon dioxide concentration using grey-box**  
2 **models**

3 Marcel Macarulla\*<sup>a</sup>, Miquel Casals<sup>a</sup>, Matteo Carnevali<sup>c</sup>, Núria Forcada<sup>a</sup>, Marta Gangoellés<sup>a</sup>

4

5 **Authors' affiliation**

6 <sup>a</sup> Universitat Politècnica de Catalunya, Department of Project and Construction Engineering,  
7 Group of Construction Research and Innovation (GRIC), C/Colom, 11, Ed. TR5, 08222  
8 Terrassa, Barcelona, Spain; <sup>b</sup> Università Politecnica delle Marche, Department of Civil and  
9 Building Engineering and Architecture, Via delle Brece Bianche, 60100 Ancona, Italy.

10

11 **Corresponding author**

12 Marcel Macarulla, PhD, Universitat Politècnica de Catalunya, Department of Project and  
13 Construction Engineering, Group of Construction Research and Innovation (GRIC), C/Colom,  
14 11, Ed. TR5, 08222 Terrassa, Barcelona, Spain, Tel.: +34 93 7398395,  
15 marcel.macarulla@upc.edu.

16

## 17 **Abstract**

18 Predictive control is the strategy that has the greatest reported benefits when it is implemented  
19 in a building energy management system. Predictive control requires low-order models to  
20 assess different scenarios and determine which strategy should be implemented to achieve a  
21 good compromise between comfort, energy consumption and energy cost. Usually, a  
22 deterministic approach is used to create low-order models to estimate the indoor CO<sub>2</sub>  
23 concentration using the differential equation of the tracer-gas mass balance. However, the use  
24 of stochastic differential equations based on the tracer-gas mass balance is not common. The  
25 objective of this paper is to assess the potential of creating predictive models for a specific  
26 room using for the first time a stochastic grey-box modelling approach to estimate future CO<sub>2</sub>  
27 concentrations. First of all, a set of stochastic differential equations are defined. Then, the  
28 model parameters are estimated using a maximum likelihood method. Different models are  
29 defined, and tested using a set of statistical methods. The approach used combines physical  
30 knowledge and information embedded in the monitored data to identify a suitable  
31 parametrization for a simple model that is more accurate than commonly used deterministic  
32 approaches. As a consequence, predictive control can be easily implemented in energy  
33 management systems.

34

35 **Keywords:** indoor air quality, ventilation, simulation, stochastic methods, CO<sub>2</sub> prediction,  
36 low-order model

37

38

39

## 40 **1 Introduction**

41 In Europe, buildings consume more energy than the industry and transportation sectors [1].  
42 They are responsible for 40% of energy consumption and 36% of CO<sub>2</sub> emissions [2]. Recent  
43 EU directives have focused on reducing operational buildings' energy consumption [3], as  
44 80–90% of energy consumption during their life cycle is produced during the operation stage  
45 [4–6].

46 Half of a building's energy consumption during the operation stage is due to heating,  
47 ventilation, and air-conditioning (HVAC) systems [7,8]. Thus, there is a great interest in  
48 developing technologies and operational strategies to improve the efficiency of these systems.  
49 Building energy management systems (BEMS) play an important role in this sense, because  
50 they can be used to apply advanced control strategies in buildings, to optimise HVAC  
51 systems.

52 Recent new approaches to optimise ventilation systems are demand-controlled [9–11]. This  
53 means that the ventilation rate varies depending on building occupation. This approach  
54 produces more savings in buildings where the occupancy is highly variable, such as  
55 institutional buildings or restaurants.

56 Generally, BEMS are rule-based. This means that the control approach is reactive [12], and  
57 future scenarios cannot be evaluated. As a consequence, BEMS cannot decide on the best  
58 strategy to ventilate a room or a building according to a set of indoor air quality and energy  
59 savings priorities. If predictive control is included in BEMS, the optimal control policy can be  
60 determined by minimizing a cost function [13]. In this way, more domains (i.e. cost, energy  
61 efficiency or indoor air quality) can be used to calculate the optimal strategy for the HVAC  
62 operation.

63 A considerable amount of research has been carried out to develop models for use in adaptive  
64 and predictive control [10,14–18]. However, most of the efforts are focused on the thermal

65 dynamics of the modelled systems and subsystems [10]. Little effort has been made in the  
66 field of predicting indoor air CO<sub>2</sub> concentration levels, and there is a lack of simple  
67 simulation tools and low-order state space models for predicting room CO<sub>2</sub> concentrations  
68 [19].

69 Usually, a deterministic approach is used to develop simple, low-order state space models for  
70 predicting room CO<sub>2</sub> concentrations [10] or calculating ventilation flow rates [20–25].  
71 However, very few studies in the field of indoor air CO<sub>2</sub> concentration address statistical  
72 approaches. This research presents the results of using the grey-box modelling method to  
73 estimate the indoor air CO<sub>2</sub> concentration in a single test room. There are two main  
74 differences between grey-box modelling and the deterministic approach. The deterministic  
75 approach only uses knowledge about physics, whilst the grey-box approach combines physics  
76 with monitored data. Another difference is that the framework of the first approach is  
77 deterministic, and the grey-box framework is stochastic. As a consequence, statistical  
78 methods can be used to obtain suitable parametrization [26].

79 This paper is structured as follows. Section 2 introduces the grey-box modelling concept.  
80 Section 3 describes the application of the theoretical method to a case study. Section 4  
81 presents and discusses the results. Finally, Section 5 contains the conclusions.

## 82 **2 Grey-box modelling**

83 A grey-box model is established using a combination of physical knowledge and information  
84 embedded in the monitored data [27]. Grey-box models are comprised of a deterministic  
85 function and a stochastic part that represents a continuous-time stochastic differential  
86 equation for the physical description of a system [28]. Finally, a discrete-time observation of  
87 the underlying physical system is needed to estimate the parameters. The combination of  
88 physical and experimental data can be used to identify suitable model parameterization [26].

89 The first step in grey modelling is to formulate a system of ordinary differential equations that  
90 represent well-known physical relationships:

$$91 \quad dX_t = f(X_t, U_t, \theta, t)dt \quad (\text{Equation 1})$$

92 where  $X_t$  is a vector of system states,  $U_t$  is a vector containing experimental data, and  $\theta$  is the  
93 vector of parameters that should be identified. To introduce variations that are not described  
94 by the deterministic model (i.e. noisy input to the system), a stochastic term is included in  
95 Equation 1 to yield the following system of a stochastic differential equation

$$96 \quad dX_t = f(X_t, U_t, \theta, t)dt + G(\theta, t)dw_t \quad (\text{Equation 2})$$

97 where  $W_t$  is a Wiener process, and  $G(\theta, t)$  is the diffusion term in the process.

98 Finally, the monitored output of the system  $Y_t$  is used to complete the state-space  
99 representation.

$$100 \quad Y_{t_k} = h(X_t, U_t, \theta, t) + e_t \quad (\text{Equation 3})$$

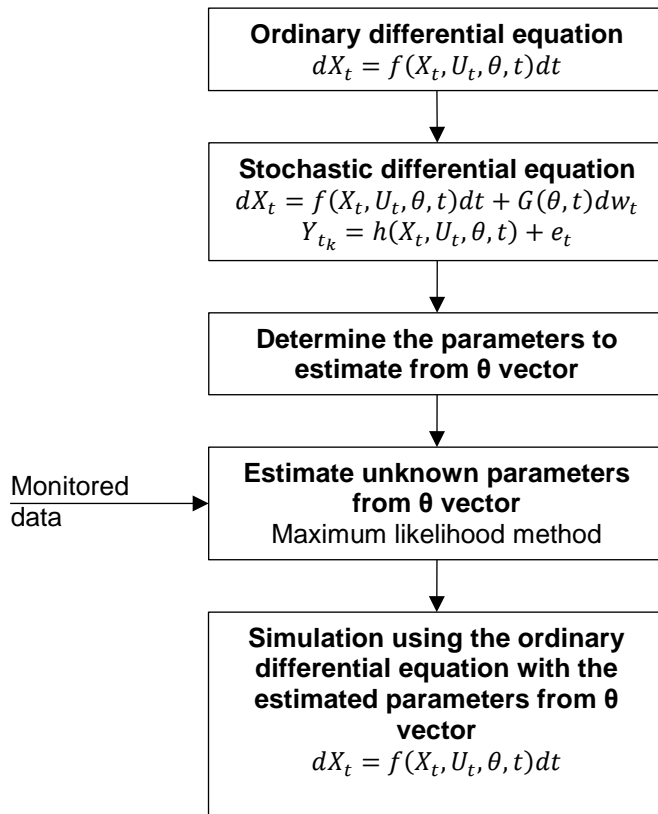
101 where function  $h(X_t, U_t, \theta, t)$  represents the relationship between the state variables and the  
102 measurements, and  $e_t$  is a vector that describes the noise from the measurements. This noise  
103 is assumed to be Gaussian distributed.

104 In order to estimate  $\theta$  in the continuous-time model, the maximum likelihood method is  
105 generally used in the literature [26–28].

106 Finally, the system of ordinary differential equations with the estimated parameters is used to  
107 carry out the simulation.

108 Grey-box modelling has been used successfully in the building sector to model the thermal  
109 energy demand of a building [26,27,29–32]. Other studies used grey-box modelling for  
110 district simulations [33].

111 Due to the minimal computational effort required by grey-box modelling and its accuracy, it  
112 is suitable for implementation in building energy management systems, for predictive control  
113 [31].



114

115 Figure 1. Grey-box modelling approach

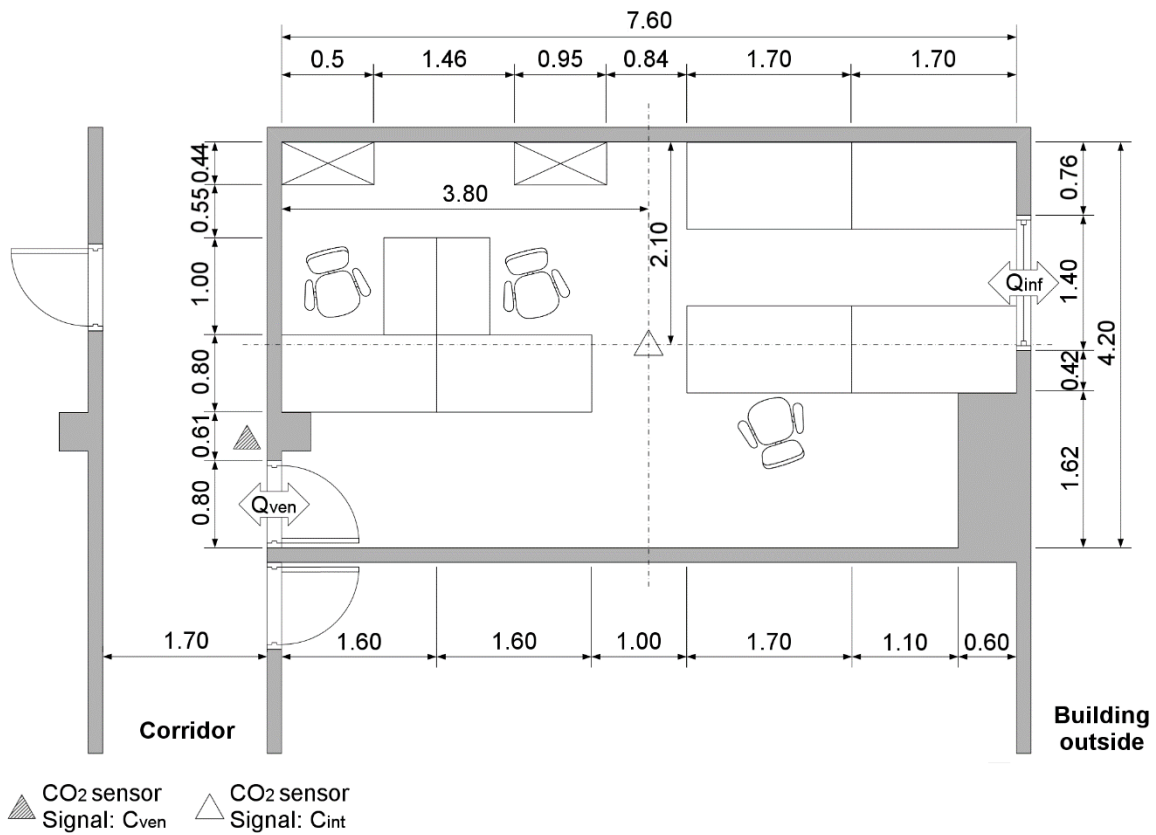
### 116 3 Methodology

117 This section presents the methodology used to study the suitability of grey-box modelling to  
 118 determine the CO<sub>2</sub> concentration in a single room.

#### 119 3.1 Data collection

120 The room was an office in TR5, an academic building on the Terrassa Campus of the  
 121 Universitat Politècnica de Catalunya (UPC). The room's surface area was 31.16 m<sup>2</sup> and its  
 122 volume was 95 m<sup>3</sup>. The maximum occupation of the room was six people, because there were  
 123 six workstations. However, the maximum occupation reached during the experimentation was  
 124 three people. The room had one window and one door providing access from the corridor.  
 125 The window measured 1.40 m long and 1.70 m high, and was positioned 1.25 m above the  
 126 floor. The room was naturally ventilated via a ventilation grill in the door. The ventilation

127 grill was rectangular and measured 0.40 m long and 0.20 m high, and was positioned 0.10 m  
 128 above the floor.



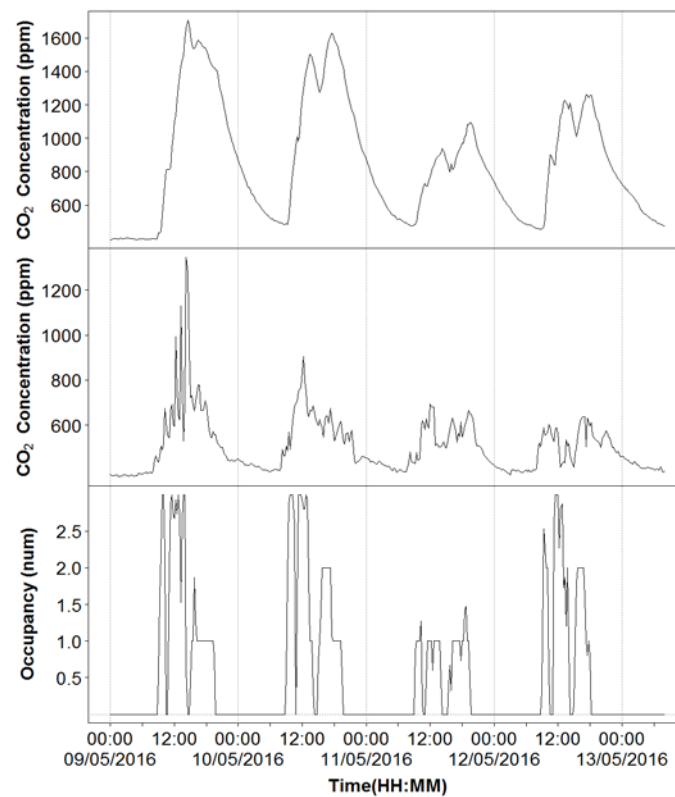
129  
 130 Figure 2. Plan view showing the positioning of sensors and objects inside the room (all  
 131 measurements are in meters)

132 The CO<sub>2</sub> concentration in the room and corridor ( $C_{int}$  and  $C_{ven}$ ) was monitored with an  
 133 Advanticsys IAQM-THCO<sub>2</sub> sensor that has a range from 0 to 3,000 ppm, a resolution of 1  
 134 ppm, and an accuracy of  $\pm 2\%$  of full-scale output. The sensor is calibrated by the  
 135 manufacturer and is configured by the manufacturer to record an instantaneous value every 15  
 136 minutes. Both sensors were located 3.00 m above the floor, under the ceiling.

137 The CO<sub>2</sub> concentration in a room with people breathing is not homogenous [10,34-36].  
 138 However, a representative measurements of CO<sub>2</sub> concentration can be effectively done in the  
 139 centre of the room [36]. For this reason, the room sensor was located in the centre of the  
 140 room.



141 An occupancy sheet was used to determine the room occupation. Each occupant noted on the  
142 sheet when they entered and left the room. The occupancy sheet was transformed into an  
143 occupation signal using the mean occupancy for each quarter of an hour.  
144 Data were collected over four days in May 2016. Figure 3 presents the data set used in this  
145 research, and Table 1 presents the indoor and outdoor air parameters during the  
146 measurements.  
147



148  
149 Figure 3. Data set. From the top, the first plot shows the CO<sub>2</sub> concentration observed inside  
150 the room, the second shows the CO<sub>2</sub> concentration observed in the corridor, and the last plot  
151 presents the occupancy of the room.

152 Table 1. Measurement conditions

Location	Parameter	Units	Value
Corridor air parameters	Average temperature	°C	23.5
	Average relative humidity	%	49
Room air parameters	Average temperature	°C	23.1
	Average relative humidity	%	51
Outdoor air parameters	Average temperature	°C	14.7
	Average relative humidity	%	82
	Average atmospheric pressure	hPa	1006.8
	Average wind speed	m/s	2.1
	CO <sub>2</sub> concentration	ppm	372

153

### 154 **3.2 Modelling process**

155 In this paper, the deterministic function is based on the principal of mass balance in a  
 156 designated volume ( $V_r$ ) [20,22,37,38]. The change in CO<sub>2</sub> concentration ( $C_{int}$ ) in the room is  
 157 expressed as:

$$158 \frac{dC_{int}}{dt} V_r = (C_{ven} - C_{int}) \cdot Q_{ven} + G_{CO_2} \quad (\text{Equation 4})$$

159 where  $V_r$  is the volume of air in the assessed room,  $C_{ven}$  is the CO<sub>2</sub> concentration of fresh air,  
 160  $C_{int}$  is the CO<sub>2</sub> concentration in the room,  $Q_{ven}$  is the ventilation rate, and  $G_{CO_2}$  is the CO<sub>2</sub>  
 161 generated by the occupants.

162 In this case,  $C_{ven}$  is assumed to be equal to the corridor's CO<sub>2</sub> because the room is ventilated  
 163 by means of a grill in the door. The  $G_{CO_2}$  is calculated using the following equation:

$$164 G_{CO_2} = K_{occ} \cdot P \quad (\text{Equation 5})$$

165 where  $K_{occ}$  is the CO<sub>2</sub> emission rate per occupant, and  $P$  is the occupancy of the room. To  
 166 complete the stochastic differential equation a stochastic term is added.

167 
$$dC_{\text{int}} = \frac{Q_{\text{ven}}}{V_r} (C_{\text{ven}} - C_{\text{int}}) \cdot dt + \frac{K_{\text{occ}} \cdot P}{V_r} \cdot dt + \sigma \cdot dw$$
 (Equation 6)

168 where  $dw$  is the Wiener process, and  $\sigma$  is the incremental variance of the Wiener process.

169 Finally, the monitored output of the system is defined in this paper by the following discrete  
170 time equation:

171 
$$Y_{t_k} = C_{\text{int}, t_k} + e_k$$
 (Equation 7)

172 where  $C_{\text{int}, t_k}$  is the measured interior CO<sub>2</sub> concentration of the room at time  $t_k$ , and  $e_k$  is the  
173 white noise process describing the measurements' noise.

174 Equation 6 assumes four hypotheses: i) CO<sub>2</sub> is chemically stable and inert, and there is no  
175 absorption process that can reduce the CO<sub>2</sub> concentration; ii) walls, ceilings and furniture do  
176 not absorb CO<sub>2</sub>; iii) the room has a perfectly mixed condition; iv) the room has a constant  
177 ventilation air flow.

178 This paper presents 4 different models to simulate the CO<sub>2</sub> concentration inside a room. The  
179 characteristics of these models are summarized in Table 2.

180

181 Table 2. Grey-box models used

Model	State space representation	Observation	Input	Estimated parameters
M1	$dC_{\text{int}} = \frac{Q_{\text{ven}}}{95} (372 - C_{\text{int}}) \cdot dt + \frac{33,800 \cdot P}{95} \cdot dt + \sigma \cdot dw$ $Y_{t_k} = C_{\text{int}, t_k} + e_k$	$C_{\text{int}}$	P	$C_{\text{int}}, Q_{\text{ven}}, \sigma, e_k$
M2	$dC_{\text{int}} = \frac{Q_{\text{ven}}}{95} (372 - C_{\text{int}}) \cdot dt + \frac{K_{\text{occ}} \cdot P}{95} \cdot dt + \sigma \cdot dw$ $Y_{t_k} = C_{\text{int}, t_k} + e_k$	$C_{\text{int}}$	P	$C_{\text{int}}, Q_{\text{ven}}, K_{\text{occ}}, \sigma, e_k$
M3	$dC_{\text{int}} = \frac{Q_{\text{ven}}}{95} (C_{\text{ven}} - C_{\text{int}}) \cdot dt + \frac{K_{\text{occ}} \cdot P}{95} \cdot dt + \sigma \cdot dw$ $Y_{t_k} = C_{\text{int}, t_k} + e_k$	$C_{\text{int}}$	P, $C_{\text{ven}}$	$C_{\text{int}}, Q_{\text{ven}}, K_{\text{occ}}, \sigma, e_k$
M4	$dC_{\text{int}} = \frac{Q_{\text{ven}}}{95} (C_{\text{ven}} - C_{\text{int}}) \cdot dt + \frac{Q_{\text{inf}}}{95} (372 - C_{\text{int}}) \cdot dt + \frac{K_{\text{occ}} \cdot P}{95} \cdot dt + \sigma \cdot dw$ $Y_{t_k} = C_{\text{int}, t_k} + e_k$	$C_{\text{int}}$	P, $C_{\text{ven}}$	$C_{\text{int}}, Q_{\text{ven}}, Q_{\text{inf}}, K_{\text{occ}}, \sigma, e_k$

182

183

184

185 The first model (M1) is used to estimate the existing ventilation in the room. The only input in  
186 the model is occupancy. The rest of the parameters are constant values. The CO<sub>2</sub>  
187 concentration of the supply air ( $C_{ven}$ ) used is 372 ppm. This value is the average reading of an  
188 external CO<sub>2</sub> sensor located outside the building. It is similar to other values obtained in other  
189 studies [39]. The human emission rate of CO<sub>2</sub> for an adult seated, reading or writing is 32,500  
190 mg/h (16.5 L/h) for a woman and 36,600 mg/h (18.6 L/h) for a man [22]. Usually, the room  
191 used to carry out the experiments is occupied by two women and one man. The value used in  
192 this research for the human emission rate of CO<sub>2</sub> is 33,900 mg/h (17.3 L/h), which is the  
193 weighted average of the aforementioned values.

194 The difference between M1 and the second model (M2) is that the human emission rate of  
195 CO<sub>2</sub> is estimated instead of a fixed rate. Model 3 (M3) added the measured CO<sub>2</sub> concentration  
196 of the supply air, the rest of the parameters remained as in M2.

197 Finally, model 4 (M4) incorporates the ventilation due to window infiltrations ( $Q_{inf}$ ). Equation  
198 6 should be modified to consider this change.

$$199 \quad dC_{int} = \frac{Q_{ven}}{V_r} (C_{ven} - C_{int}) \cdot dt + \frac{Q_{inf}}{V_r} (C_{inf} - C_{int}) \cdot dt + \frac{K_{occ} \cdot P}{V_r} \cdot dt + \sigma \cdot dw \quad (\text{Equation 8})$$

200 The parameters of the assessed grey-box models are estimated using the CTSM-R Version  
201 1.0.0 package for an R environment. This package uses the maximum likelihood and Kalman  
202 filtering for the estimations [40]. A 2.50-GHz Intel Core i7 personal computer was used to  
203 carry out the estimations.

### 204 **3.3 Model validation**

205 This paper proposes a set of models to estimate CO<sub>2</sub> concentrations in indoor spaces, based  
206 partially on the physical characteristics of the system. Consequently, the first step in the  
207 model validation process is to check whether the estimated parameters are feasible in terms of  
208 the physics of the system [27–30]. The estimated parameters are compared with the literature  
209 and the ASHRAE standard.

210 Then, using all the data set, a set of statistical tests are used to determine whether the  
211 estimated parameter values describe the dynamics of the system. The statistical tests and the  
212 model validation process are based on previous studies [27–29].

213 The first statistical test is the assessment of parameter significance. The probability value of  
214 the parameters should be less than 0.05, otherwise the parameter is insignificant [40]. Then,  
215 the derivative of the objective function compared to the particular initial state or parameter is  
216 assessed. If the values that are obtained are not close to zero, the solution may be a local  
217 optimum, but not the true optimum [41]. Subsequently, the derivative of the penalty function  
218 with respect to the particular initial state or parameters is assessed. If this value is significant  
219 compared to the derivative of the objective function with respect to the particular initial state  
220 or parameter, the particular initial state or parameter may be close to one of its limits. Then,  
221 the estimation should be repeated with new limits [40]. The correlation matrix of the  
222 parameter estimates is also calculated to ensure that off-diagonal values are far from 1 or -1.  
223 Values on the off-diagonal that are near to 1 or -1 indicate that the model is over-  
224 parametrized. Then, the elimination of some model parameters should be taken into  
225 consideration [40].

226 The assumption of white noise residuals is assessed with the autocorrelation function and the  
227 cumulated periodogram [27,28]. Finally, the root mean square error deviation is used to assess  
228 whether the calculated model can predict the system with reasonable accuracy. All the  
229 aforementioned statistical tests are provided by the CTSM-R package.

## 230 **4 Results and discussion**

231 All the estimated parameters of all the models reported reasonable values. The estimated  
232 ventilation flows ranged between 20.13 m<sup>3</sup>/h and 92.16 m<sup>3</sup>/h. These values are lower than  
233 established by the standards. This is an expected result, because the room only has natural  
234 ventilation through the corridor. In addition, the CO<sub>2</sub> concentration reaches and surpasses

235 1000 ppm during working hours. The RMSE of the assessed models ranges between 41.09  
236 and 370.67 ppm. However, only one model can be considered statistically relevant.  
237 The estimation of the ventilation flow rate obtained with M1 is reasonable (24.40 m<sup>3</sup>/h). The  
238 p-value of the t-test is below 0.05 in all estimated parameters, except e. However, this  
239 parameter is not important for the resultant model and this value can be accepted. The  
240 derivative of the objective function with respect to each parameter is close to 0 and the  
241 derivative function with respect to each parameter is not significant compared to dF/dPar  
242 (Table 3 and Table 4). The autocorrelation plot shows that the residues are not random,  
243 because most of the autocorrelations are outside of the 95% confidence bands. The values of  
244 the cumulated periodogram are outside of the 95% confidence bands (Figure 4). As a  
245 consequence, is not possible to affirm that the residuals obtained can be regarded as white  
246 noise. The model follows the trend, however it overestimates the peaks and underestimates  
247 the lower values. The RMSE is 370.67 ppm, the highest of the four models. According to the  
248 results, this model cannot be considered useful to simulate the CO<sub>2</sub> inside the room.

249 Table 3. Statistical tests for M1

Parameter	Estimation	Standard error	Pr(> t )	dF/dPar	dPen/dPar
$C_{int}$	393	45	0.000	1.9346E-05	1.9346E-05
$Q_{vent}$	24.40	0.18	0.000	5.5770E-03	5.5770E-03
$\sigma$	96.54	0.03	0.000	-4.9756E-06	1.1645E-03
e	0.00	49.23	8.200	1.1645E-03	-4.9756E-06

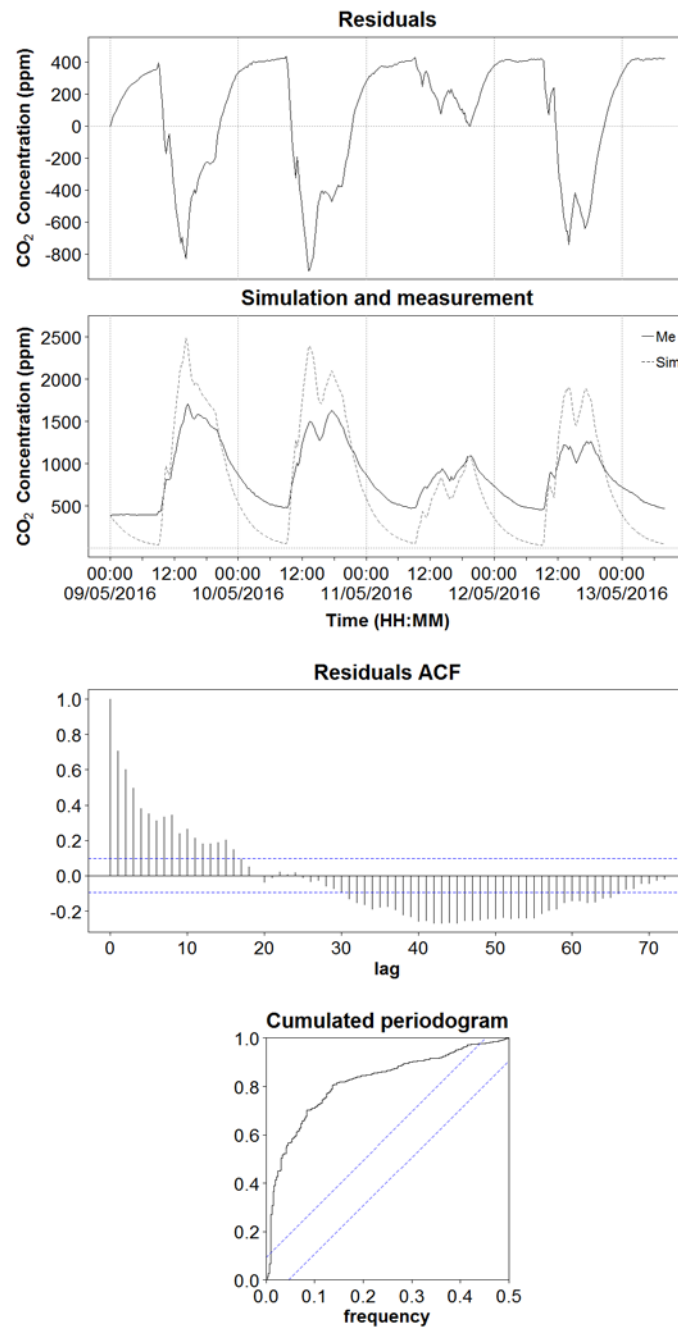
250

251 Table 4. Correlation coefficients for M1

	$C_{int}$	$Q_{vent}$	E
$Q_{vent}$	0.01		
e	-0.02	-0.71	
$\sigma$	-0.04	-0.06	0.17

252





253

254 Figure 4. On the upper left, the residuals plot for M1 is presented; on the bottom left, the  
 255 measured data compared to the simulated data for M1 is plotted. On the top right, the  
 256 autocorrelation function (ACF) for the residuals of M1 is plotted, and on the bottom right the  
 257 cumulated periodogram for M1 is presented.

258 M2 reported similar results to M1. The statistical parameters were all inside the acceptable  
 259 range (Table 5 and Table 6), but the autocorrelation function and the cumulated periodogram

260 were out of the 95% confidence bands (Figure 5). The root mean square error of this model  
 261 was 156.34 ppm. The human emission rate of CO<sub>2</sub> estimated by the model is 62% lower than  
 262 that established in the literature. However, this result cannot be taken into account, because  
 263 the results of statistical tests recommend discarding this model.

264

265 Table 5. Statistical tests for M2

Parameter	Estimation	Standard error	Pr(> t )	dF/dPar	dPen/dPar
C <sub>int</sub>	393	16	0.000	-5.9627E-06	0.0000E+00
Q <sub>vent</sub>	92.16	0.45	0.000	-5.8693E-06	0.0000E+00
K <sub>occ</sub>	12,862	370	0.000	2.6688E-05	0.0000E+00
$\sigma$	33.45	0.04	0.000	-9.2872E-06	0.0000E+00
e	0.00	262.39	0.971	-5.3579E-06	1.0000E-04

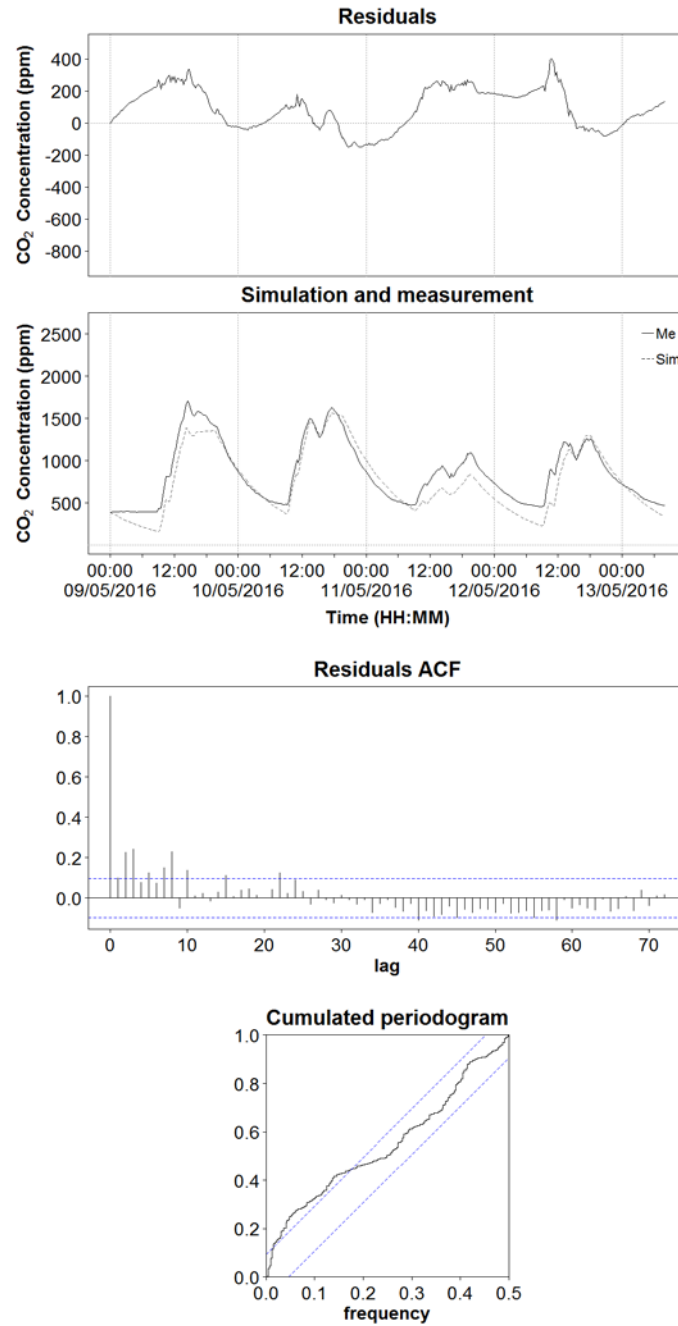
266

267 Table 6. Correlation coefficients for M2

	C <sub>int</sub>	Q <sub>vent</sub>	K <sub>occ</sub>	$\sigma$
Q <sub>vent</sub>	0.01			
K <sub>occ</sub>	0.03	0.62		
$\sigma$	-0.01	0.03	0.06	
e	0.00	0.00	0.00	0.00

268

269



270

271 Figure 5. On the upper left, the residuals plot for M2 is presented; on the bottom left, the  
 272 measured data compared to the simulated data for M2 is plotted. On the top right, the ACF for  
 273 the residuals for M2 is plotted, and on the bottom right the cumulated periodogram for M2 is  
 274 presented.

275

276 The best results are those of M3. The estimated values are reasonable (Table 7). The  
277 estimated ventilation flow rate is  $20.13 \text{ m}^3/\text{h}$  ( $0.21 \text{ h}^{-1}$ ). This value is similar to the results of  
278 similar research. For example, a study of the natural ventilation in college student dormitories  
279 reported an air change rate above  $0.5 \text{ h}^{-1}$  [20]. Another study related with ventilation in a  
280 commercial building reported an air change rate of  $0.1 \text{ h}^{-1}$  [21]. According to the ASHRAE  
281 handbook, the required minimum ventilation for the assessed room should be  $121.31 \text{ m}^3/\text{h}$ ,  
282 taking into account that no more than six people are expected to occupy the area for its  
283 normal use. The human emission rate of  $\text{CO}_2$  estimated by the model is  $12,793 \text{ mg/h}$  ( $6.5$   
284  $\text{L/h}$ ). According to the literature [22], the human emission rate of  $\text{CO}_2$  for an adult who is  
285 seated or reading or writing is  $32,500 \text{ mg/h}$  ( $16.5 \text{ L/h}$ ) for a female and  $36,600 \text{ mg/h}$  ( $18.6$   
286  $\text{L/h}$ ) for a male. The value of the human emission rate of  $\text{CO}_2$  is 62% lower than the  
287 reference. As reported by other studies in the field [22], the reference value is calculated using  
288 a hypothesis that cannot be true for this case. However, the estimated value has the same  
289 order of magnitude.

290 All the statistical tests calculated for M3 are inside the boundaries (Table 7 and Table 8). In  
291 addition, values of the autocorrelation plot and the cumulated periodogram are inside of the  
292 95% confidence bands (Figure 6). As a consequence, the residuals obtained can be regarded  
293 as white noise. The root mean square error for the third model was  $41.10 \text{ ppm}$ . This value is  
294 lower than that found in other studies presented in the literature that used deterministic  
295 approaches, such as Pantazaras study [10] who reported a RMSE ranging from 50 to 60 ppm.  
296 The accuracy of the reported model in this research is sufficient, because it is close to the  
297 accuracy of most commercial  $\text{CO}_2$  sensors. In this case, taking into account that the accuracy  
298 of the sensors is  $\pm 2\%$  of full scale, the accuracy of the sensor is  $\pm 60 \text{ ppm}$ .

299

300

301

302 Table 7. Statistical tests for M3

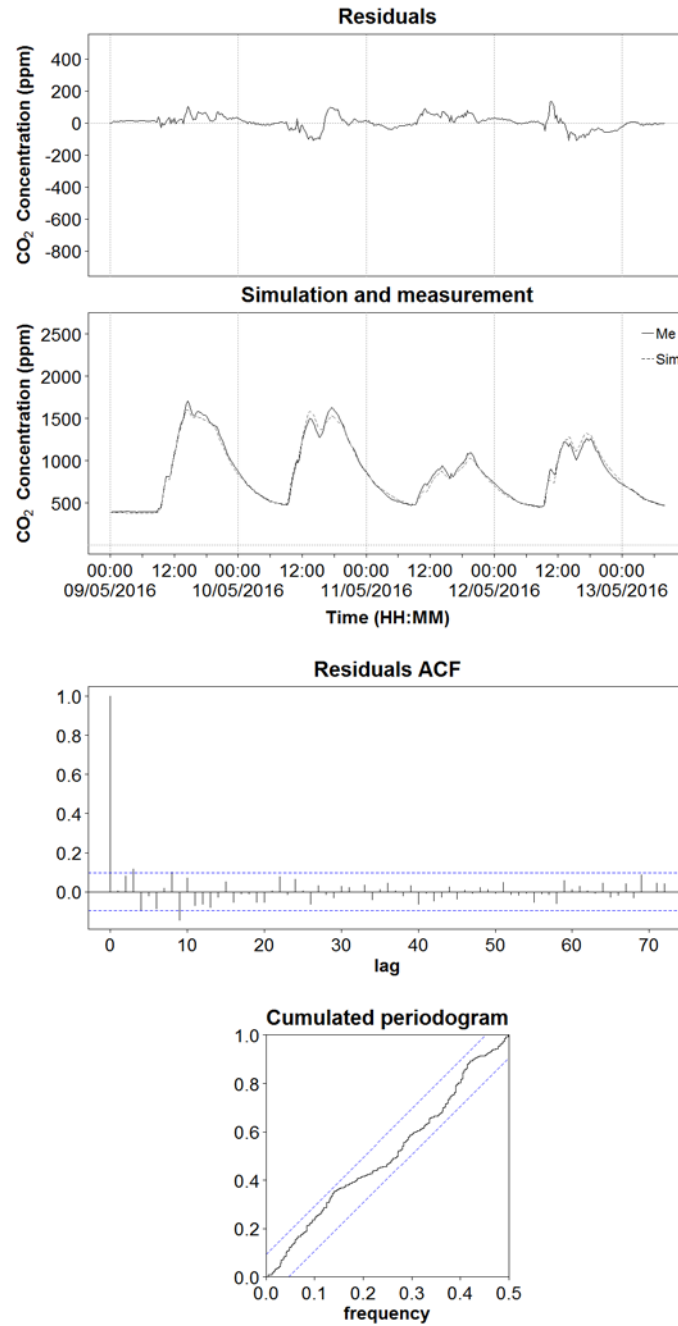
Parameter	Estimation	Standard error	Pr(> t )	dF/dPar	dPen/dPar
$C_{int}$	393	14	0.000	0.0000E+00	0.0000E+00
$Q_{vent}$	20.13	0.71	0.000	-3.6668E-06	0.0000E+00
$K_{occ}$	12,793	306	0.000	0.0000E+00	0.0000E+00
$\sigma$	27.66	0.06	0.000	-9.2670E-06	0.0000E+00
e	13.33	0.75	0.001	6.8335E-06	0.0000E+00

303

304 Table 8. Correlation coefficients for M3

	$C_{int}$	$Q_{vent}$	$K_{occ}$	$\sigma$
$Q_{vent}$	-0.04			
$K_{occ}$	-0.03	0.57		
$\sigma$	-0.02	-0.02	-0.10	
e	0.02	0.05	0.13	-0.73

305



306

307 Figure 6. On the upper left, the residuals plot for M3 is presented; on the bottom left, the  
 308 measured data compared to the simulated data for M3 is plotted. On the top right, the ACF for  
 309 residuals for M3 is plotted, and on the bottom right the cumulated periodogram for M3 is  
 310 presented.

311

312 The last model (M4) reported a similar value of the root mean square error to M3 (41.18  
 313 ppm). However, statistical tests showed that the parameter window infiltrations are not  
 314 relevant for the model (Table 9 and Table 10). Therefore, the fourth model is discarded.  
 315 Generally, in the literature, infiltrations are unified with the supply air [10]. The results of this  
 316 research enable us to affirm that the approximation generally used in the literature is  
 317 acceptable. Further research considering measured external CO<sub>2</sub> should be carried out to  
 318 affirm that infiltrations are not relevant to model the internal CO<sub>2</sub> concentration in buildings  
 319 with good air tightness.

320

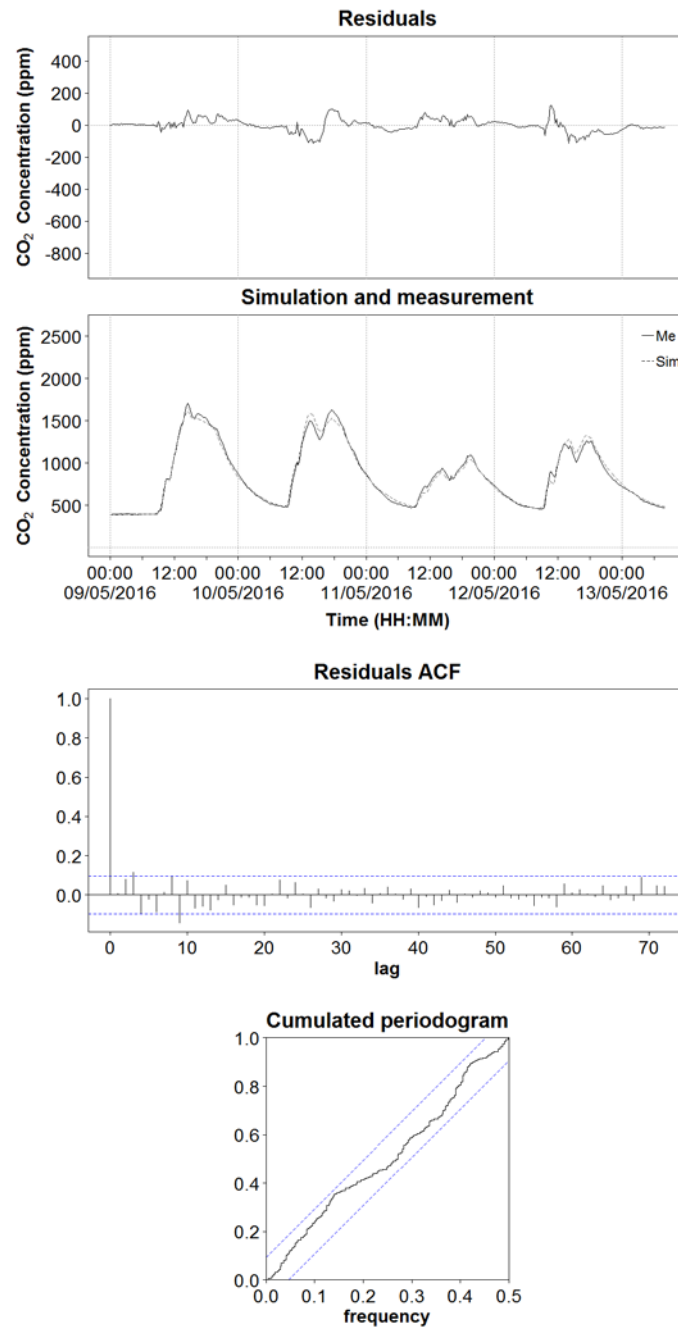
321 Table 9. Statistical tests for M4

Parameter	Estimation	Standard error	Pr(> t )	dF/dPar	dPen/dPar
C <sub>int</sub>	393	13	0.000	-2.9813E-06	0.0000E+00
Q <sub>vent</sub>	20.10	0.78	0.000	-4.1809E-05	0.0000E+00
Q <sub>inf</sub>	0.00	0.01	0.996	4.0135E-05	0.0000E+00
K <sub>occ</sub>	12,748	330	0.0000E+00	6.1870E-05	0.0000E+00
σ	29.67	0.04	0.0000E+00	-1.8548E-04	0.0000E+00
e	0.00	126.39	0.910	8.2055E-04	8.0000E-04

322

323 Table 10. Correlation coefficients for M4

	C <sub>int</sub>	Q <sub>vent</sub>	Q <sub>inf</sub>	K <sub>occ</sub>	σ
Q <sub>vent</sub>	0.00				
Q <sub>inf</sub>	0.00	-0.02			
K <sub>occ</sub>	0.00	-0.55	0.00		
σ	-0.02	0.07	0.00	0.10	
e	0.00	-0.02	1	0.00	0.00



325

326 Figure 7. On the upper left, the residuals plot for M4 is presented; on the bottom left the  
 327 measured data in front of simulated data for M4 is plotted. On the top right, the ACF for the  
 328 residuals for M4 is plotted, and on the bottom right the cumulated periodogram for M4 is  
 329 presented.



330 The average computation time needed to carry out the estimation of the parameters, the  
331 statistical tests and the simulations for the current dataset was less than 3 seconds for each  
332 model.

## 333 **5 Conclusions**

334 This study investigated the possibility of using grey-box modelling for the CO<sub>2</sub> concentration  
335 in a room. The procedure proposed in this paper for modelling indoor air CO<sub>2</sub> concentration is  
336 formulated as a system of stochastic differential equations. To identify the parameters of each  
337 model, the maximum likelihood method is used. The models are validated using a set of  
338 statistical methods and physical interpretation of the estimated parameters. With these  
339 arguments, the best model is identified.

340 The main contribution of this paper is a new approach to model the indoor CO<sub>2</sub> concentration  
341 in a specific room, which could be broadened to entire buildings in the future. The proposed  
342 approach enables to obtain more accurate and simplistic models to simulate indoor CO<sub>2</sub> than  
343 currently applied deterministic approaches.

344 The results of this research demonstrated that once a model has been identified for a specific  
345 room, the CO<sub>2</sub> concentration can be modelled inside the room using the occupancy, the  
346 ventilation rate, and the CO<sub>2</sub> concentration of the ventilation air flow.

347 The results of this research can be used to implement a tool in a BEMS to analyse the existing  
348 levels of ventilation in a building. In this way, we can detect which rooms are under-  
349 ventilated or over-ventilated, and the building maintenance team can then investigate any  
350 potential problems. When the system is parametrized, a predictive control strategy can be  
351 implemented in a BEMS to optimize the building ventilation system. However, before  
352 implementing predictive control, the accuracy of different prediction horizons should be  
353 assessed.

354 Further research is required to investigate whether the proposed approach can be used to  
355 configure a model and determine the occupancy of a room when we know the CO<sub>2</sub>  
356 concentration in the room, the ventilation rate, and the CO<sub>2</sub> concentration of the ventilation air  
357 flow. As a result, a service could be implemented in a BEMS to estimate the occupancy of a  
358 room.

359 The approach used one CO<sub>2</sub> sensor to estimate the model parameters. In this case, a perfect,  
360 mixed condition in the room is assumed. Extreme care should be taken when the location of a  
361 CO<sub>2</sub> sensor is selected, due to the highly localised nature of indoor CO<sub>2</sub> concentrations. For  
362 this reason, further research is required to determine how many sensors are needed to estimate  
363 ventilation parameters with an acceptable level of accuracy. In addition, the optimal position  
364 of sensors should be studied.

365 Another aspect that should be studied in the future is the difference between the value of the  
366 human emission rate of CO<sub>2</sub> obtained using grey-box modelling, and the value generally used  
367 in the literature.

## 368 **References**

- 369 [1] H.S. Park, M. Lee, H. Kang, T. Hong, J. Jeong, Development of a new energy  
370 benchmark for improving the operational rating system of office buildings using  
371 various data-mining techniques, *Appl. Energy*. 173 (2016) 225–237.  
372 doi:10.1016/j.apenergy.2016.04.035.
- 373 [2] European comission, Financial support for energy efficiency in buildings, Report from  
374 the Commision to the European parliament and the Council, 2013.  
375 [https://ec.europa.eu/energy/sites/ener/files/documents/report\\_financing\\_ee\\_buildings\\_c  
376 om\\_2013\\_225\\_en.pdf](https://ec.europa.eu/energy/sites/ener/files/documents/report_financing_ee_buildings_com_2013_225_en.pdf).
- 377 [3] M. Iten, S. Liu, A. Shukla, A review on the air-PCM-TES application for free cooling  
378 and heating in the buildings, *Renew. Sustain. Energy Rev.* 61 (2016) 175–186.

- 379 doi:10.1016/j.rser.2016.03.007.
- 380 [4] A. Atmaca, N. Atmaca, Life cycle energy (LCEA) and carbon dioxide emissions  
381 (LCCO2A) assessment of two residential buildings in Gaziantep, Turkey, *Energy*  
382 *Build.* 102 (2015) 417–431. doi:10.1016/j.enbuild.2015.06.008.
- 383 [5] K.I. Praseeda, B.V.V. Reddy, M. Mani, Embodied and operational energy of urban  
384 residential buildings in India, *Energy Build.* 110 (2016) 211–219.  
385 doi:10.1016/j.enbuild.2015.09.072.
- 386 [6] B. Whitehead, D. Andrews, A. Shah, G. Maidment, Assessing the environmental  
387 impact of data centres part 2: Building environmental assessment methods and life  
388 cycle assessment, *Build. Environ.* 93 (2015) 395–405.  
389 doi:10.1016/j.buildenv.2014.08.015.
- 390 [7] J. Hu, P. Karava, A state-space modeling approach and multi-level optimization  
391 algorithm for predictive control of multi-zone buildings with mixed-mode cooling,  
392 *Build. Environ.* 80 (2014) 259–273. doi:10.1016/j.buildenv.2014.05.003.
- 393 [8] H. Huang, L. Chen, E. Hu, A new model predictive control scheme for energy and cost  
394 savings in commercial buildings: An airport terminal building case study, *Build.*  
395 *Environ.* 89 (2015) 203–216. doi:10.1016/j.buildenv.2015.01.037.
- 396 [9] M. Macarulla, M. Albano, L.L. Ferreira, C. Teixeira, Lessons Learned in Building a  
397 Middleware for Smart Grids, *J. Green Eng.* 6 (2016) 1–26. doi:10.13052/jge1904-  
398 4720.611.
- 399 [10] A. Pantazaras, S.E. Lee, M. Santamouris, J. Yang, Predicting the CO2 levels in  
400 buildings using deterministic and identified models, *Energy Build.* 127 (2016) 774–  
401 785. doi:10.1016/j.enbuild.2016.06.029.
- 402 [11] A. Leavey, Y. Fu, M. Sha, A. Kutta, C. Lu, W. Wang, et al., Air quality metrics and  
403 wireless technology to maximize the energy efficiency of HVAC in a working

- 404 auditorium, *Build. Environ.* 85 (2015) 287–297. doi:10.1016/j.buildenv.2014.11.039.
- 405 [12] D. Kolokotsa, A. Pouliezos, G. Stavrakakis, C. Lazos, Predictive control techniques for  
406 energy and indoor environmental quality management in buildings, *Build. Environ.* 44  
407 (2009) 1850–1863. doi:10.1016/j.buildenv.2008.12.007.
- 408 [13] M. Vaccarini, A. Giretti, L.C. Tolve, M. Casals, Model predictive energy control of  
409 ventilation for underground stations, *Energy Build.* 116 (2016) 326–340.  
410 doi:10.1016/j.enbuild.2016.01.020.
- 411 [14] D.W.U. Perera, D. Winkler, N.-O. Skeie, Multi-floor building heating models in  
412 MATLAB and Modelica environments, *Appl. Energy.* 171 (2016) 46–57.  
413 doi:10.1016/j.apenergy.2016.02.143.
- 414 [15] M. Dahl Knudsen, S. Petersen, Demand response potential of model predictive control  
415 of space heating based on price and carbon dioxide intensity signals, *Energy Build.* 125  
416 (2016) 196–204. doi:10.1016/j.enbuild.2016.04.053.
- 417 [16] C.C. Menassa, N. Taylor, J. Nelson, Optimizing hybrid ventilation in public spaces of  
418 complex buildings – A case study of the Wisconsin Institutes for Discovery, *Build.*  
419 *Environ.* 61 (2013) 57–68. doi:10.1016/j.buildenv.2012.12.009.
- 420 [17] H.B. Gunay, J. Bursill, B. Huchuk, W. O’Brien, I. Beausoleil-Morrison, Shortest-  
421 prediction-horizon model-based predictive control for individual offices, *Build.*  
422 *Environ.* 82 (2014) 408–419. doi:10.1016/j.buildenv.2014.09.011.
- 423 [18] Y. Yu, V. Loftness, D. Yu, Multi-structural fast nonlinear model-based predictive  
424 control of a hydronic heating system, *Build. Environ.* 69 (2013) 131–148.  
425 doi:10.1016/j.buildenv.2013.07.018.
- 426 [19] J.C. Salcido, A.A. Raheem, R.R.A. Issa, From simulation to monitoring: Evaluating the  
427 potential of mixed-mode ventilation (MMV) systems for integrating natural ventilation  
428 in office buildings through a comprehensive literature review, *Energy Build.* 127

- 429 (2016) 1008–1018. doi:10.1016/j.enbuild.2016.06.054.
- 430 [20] H. Li, X. Li, M. Qi, Field testing of natural ventilation in college student dormitories  
431 (Beijing, China), *Build. Environ.* 78 (2014) 36–43.  
432 doi:10.1016/j.buildenv.2014.04.009.
- 433 [21] L.C. Ng, J. Wen, Estimating building airflow using CO<sub>2</sub> measurements from a  
434 distributed sensor network, *HVAC&R Res.* 17 (2011) 344–365.  
435 doi:10.1080/10789669.2011.572223.
- 436 [22] W. Zhang, L. Wang, Z. Ji, L. Ma, Y. Hui, Test on Ventilation Rates of Dormitories and  
437 Offices in University by the CO<sub>2</sub> Tracer Gas Method, in: *Procedia Eng.*, Elsevier,  
438 2015: pp. 662–666. doi:10.1016/j.proeng.2015.08.1061.
- 439 [23] K.W. Cheong, Airflow measurements for balancing of air distribution system — tracer-  
440 gas technique as an alternative?, *Build. Environ.* 36 (2001) 955–964.  
441 doi:10.1016/S0360-1323(00)00046-9.
- 442 [24] S. Cui, M. Cohen, P. Stabat, D. Marchio, CO<sub>2</sub> tracer gas concentration decay method  
443 for measuring air change rate, *Build. Environ.* 84 (2015) 162–169.  
444 doi:10.1016/j.buildenv.2014.11.007.
- 445 [25] M. Labat, M. Woloszyn, G. Garnier, J.J. Roux, Assessment of the air change rate of  
446 airtight buildings under natural conditions using the tracer gas technique. Comparison  
447 with numerical modelling, *Build. Environ.* 60 (2013) 37–44.  
448 doi:10.1016/j.buildenv.2012.10.010.
- 449 [26] K.K. Andersen, H. Madsen, L.H. Hansen, Modelling the heat dynamics of a building  
450 using stochastic differential equations, *Energy Build.* 31 (2000) 13–24.  
451 doi:10.1016/S0378-7788(98)00069-3.
- 452 [27] P. Bacher, H. Madsen, Identifying suitable models for the heat dynamics of buildings,  
453 *Energy Build.* 43 (2011) 1511–1522. doi:10.1016/j.enbuild.2011.02.005.

- 454 [28] A. Thavlov, H. Madsen, A non-linear stochastic model for an office building with air  
455 infiltration, *Int. J. Sustain. Energy Plan. Manag.* 7 (2015) 55–66.  
456 doi:10.5278/IJSEPM.2015.7.5.
- 457 [29] N.R. Kristensen, H. Madsen, S.B. Jørgensen, Parameter estimation in stochastic grey-  
458 box models, *Automatica*. 40 (2004) 225–237. doi:10.1016/j.automatica.2003.10.001.
- 459 [30] H. Madsen, J. Holst, Estimation of continuous-time models for the heat dynamics of a  
460 building, *Energy Build.* 22 (1995) 67–79. doi:10.1016/0378-7788(94)00904-X.
- 461 [31] G. Reynders, J. Diriken, D. Saelens, Quality of grey-box models and identified  
462 parameters as function of the accuracy of input and observation signals, *Energy Build.*  
463 82 (2014) 263–274. doi:10.1016/j.enbuild.2014.07.025.
- 464 [32] X. Li, J. Wen, Building energy consumption on-line forecasting using physics based  
465 system identification, *Energy Build.* 82 (2014) 1–12.  
466 doi:10.1016/j.enbuild.2014.07.021.
- 467 [33] R. Baetens, D. Saelens, Modelling uncertainty in district energy simulations by  
468 stochastic residential occupant behaviour, *J. Build. Perform. Simul.* 9 (2016) 431–447.  
469 doi:10.1080/19401493.2015.1070203.
- 470 [34] N. Mahyuddin, H. Awbi, The spatial distribution of carbon dioxide in an environmental  
471 test chamber, *Build. Environ.* 45 (2010) 1993–2001.  
472 doi:10.1016/j.buildenv.2010.02.001.
- 473 [35] N. Mahyuddin, H.B. Awbi, M. Alshitawi, The spatial distribution of carbon dioxide in  
474 rooms with particular application to classrooms, *Indoor Built Environ.* 23 (2014) 433–  
475 448. doi:10.1177/1420326X13512142.
- 476 [36] A. Bulińska, Z. Popiołek, Z. Buliński, Experimentally validated CFD analysis on  
477 sampling region determination of average indoor carbon dioxide concentration in  
478 occupied space, *Build. Environ.* 72 (2014) 319–331.

- 479 doi:10.1016/j.buildenv.2013.11.001.
- 480 [37] F.D. Heidt, H. Werner, Microcomputer-aided measurement of air change rates, *Energy*  
481 *Build.* 9 (1986) 313–320. doi:10.1016/0378-7788(86)90036-8.
- 482 [38] D. Laussmann, D. Helm, Air Change Measurements Using Tracer Gases: Methods and  
483 Results. Significance of air change for indoor air quality, in: *Chem. Emiss. Control.*  
484 *Radioact. Pollut. Indoor Air Qual.*, InTech, 2011. doi:10.5772/18600.
- 485 [39] E. Specht, T. Redemann, N. Lorenz, Simplified mathematical model for calculating  
486 global warming through anthropogenic CO<sub>2</sub>, *Int. J. Therm. Sci.* 102 (2016) 1–8.  
487 doi:10.1016/j.ijthermalsci.2015.10.039.
- 488 [40] CTSM-R Development Team, Continuous Time Stochastic Modeling in R User's  
489 Guide and Reference Manual, 2015. <http://ctsm.info/>.
- 490 [41] CTSM-R Development Team, Grey-box modeling of the heat dynamics of a building  
491 with CTSM-R, 2013. <http://ctsm.info/>.